Exopolysaccharide produced by potential probiotic Enterococcus faecium MS79: characterization, bioactivities and rheological properties influenced by salt and pH

Exopolysaccharide produced by potential probiotic *Enterococcus faecium* MS79: Characterization, bioactivities and rheological properties influenced by salt and pH

Mutamed Ayyash[a]*, Constantinos Stathopoulos[a], Basim Abu-Jdayil[b]*, Gennaro Esposito[c], Mohammad Baig[a], Mark Turner[d], Ahmad Baba[e], Vasso Apostolopoulos[f], Anas Al-Nabulsi[g], Tareq Osaili[g,h]

[a] Department of Food, Nutrition and Health, College of Food and Agriculture, United Arab Emirates University (UAEU), Al Ain, UAE

[b] Chemical and Petroleum Engineering Department, College of Engineering, United Arab Emirates University (UAEU), Al Ain, UAE

[c] Science Division - New York University Abu Dhabi, NYUAD Campus, Saadiyat Island, Abu Dhabi, U

[d] School of Agriculture and Food Sciences, The University of Queensland (UQ), Brisbane, Australia

[e] Division of Biochemistry, Institute of Biological Sciences, Faculty of Science, University of Malaya, Malaysia

[f] Institute for Health and Sport, Victoria University, Melbourne, VIC, Australia

[g] Department of Nutrition and Food Technology, Jordan University of Science and Technology, Irbid, Jordan

[h] Department: Clinical Nutrition and Dietetics, University of Sharjah, Sharjah, UAE

***Corresponding authors:**
Dr. Mutamed Ayyash
Department of Food, Nutrition and Health
College of Food & Agriculture, UAEU
Tel.: +971 3 713 4552, Fax: +971 3 767 5336
Email: mutamed.ayyash@uaeu.ac.ae

Prof. Basim Abu-Jdayil
Chemical and Petroleum Engineering Department
College of Engineering, UAEU
Tel.: +971 3 713 5317
Email: Babujdayil@uaeu.ac.ae

Declarations of interest: none

Abstract

The microbial exopolysaccharide (EPS) gains escalated attention by researchers and industries. Therefore, the objectives of this study were to: 1) isolate, purify and characterize EPS produced by *Enterococcus faecium* MS79 (EPS-MS79) including molecular weight, monosaccharide composition, potential structure by NMR analyses, functional groups by FTIR, particle size and zeta potential, and thermal properties by DSC. 2) investigate bioactive properties of EPS-MS79 namely antioxidant by DPPH and ABTS, antidiabetic, antipathogenic, and anticancer activities. 3) investigate the rheological properties of the EPS-MS79 as influenced by salt type and pH level.

The average Mw of the EPS-MS79 was 8.3 x 10^5 Da. EPS-MS79 composed of three monosaccharides arabinose, mannose, and glucose in a molar ratio of 0.8:1.7:11.3. The proposed backbone structure of EPS-MS79 was: →4)[α-d-Gal(1→4)α-d-Glc(1→3)α-d-Glc(1→2)]β-d-Man(1→2)α-d-Glc(1→6)α-d-Glc(1→. Scavenging activities of EPS-MS79 were 76% and 85% as measured by DPPH and 26% and 44% as measured by ABTS. The antiproliferative activities against colon (72% and 77%) and breast (43% and 56%) cancer cell lines. The reductions in the pathogens' population were 2.7, 3.0, 3.0 and 2.9 logs CFU/mL for *S. aureus*, *S.* Typhimurium, *L. monocytogenes*, and *E. coli* O157:H7, respectively. All EPS-MS79 solutions displayed shear thinning behavior. The G' and G'' moduli of all EPS-MS79 solutions increased alongside with frequency increase. Salt type and pH level had noteworthy impact on the rheological properties of EPS-MS79. The EPS-MS79 could be a potent prebiotic promoting health and rheological properties.

1. Introduction

Polysaccharides are used widely in the food industry as thickeners emulsifiers or stabilizers, due to their ability to influence viscosity and rheology (Caggianiello, Kleerebezem, & Spano, 2016; Hussain et al., 2017). Applications in the dairy industry are particularly extensive and have been recently reviewed (Llamas-Arriba et al., 2019). However, recent studies regarding exopolysaccharides (EPS), highlight that they possess a number of underlying physiological functions and biological activities such as antioxidant, antibacterial, antiviral, antitumor, immunoregulatory, hypoglycaemic, antihypertensive and cholesterol lowering, whilst promoting the colonization of probiotics in the host (Xu et al., 2019; Zhou, Cui, & Qu, 2019).

EPS are high molecular weight carbohydrate polymers that can be further classified as either homo- or hetero-polysaccharides depending on whether they comprise a mixture of glucose, fructose, rhamnose and glucose or only a single type of monosaccharide respectively (Jiang & Yang, 2018; Monsan et al., 2001). Functionality-enhancing probiotic EPS are commonly produced by a range of Lactic Acid bacteria (LAB) as well as bifidobacteria (Llamas-Arriba et al., 2019). LABs are particularly suited for applications in the food industry due to their GRAS (generally recognized as safe) status (Saadat, Khosroushahi, & Gargari, 2019; Xu et al., 2019). Numerous studies have shown the physicochemical characteristics and bioactivates of EPS produced by Lactobacilli (Zhou et al., 2019) and particularly *Lactobacillus plantarum* (Jiang & Yang, 2018; Silva, Lopes Neto, & Cardarelli, 2019), *L. bulgaricus* RR (Kimmel, Roberts, & Ziegler, 1998) and *Bifidobacterium longum BB-79* (Roberts et al., 1995; Xu et al., 2019) *Enterococcus faecium*, a Gram-positive bacterium formerly of the group D Streptococci system, known as *Streptococcus faecium* (Ryan & Ray, 2004). *E. faecium* is of particular interest as it is a

known extremophile, able to tolerate very basic conditions (pH 9.6) and very high salt concentrations (Nicolaus, Kambourova, & Oner, 2010). Unlike *L. plantarum*, few attempts have studied the properties of EPS produced by *E. faecium* isolated from infants (Jia et al., 2019), fermented milk product (Bhat & Bajaj, 2018), fresh and processed fish products (Abdhul et al., 2014; Kanmani et al., 2013). However, these reports have a limited focusing on the biological activities namely antioxidant, hypocholesterolaemia, and antibiofilm. Therefore, the present study is a comprehensive analysis of bioactivities and their rheological properties of EPS produced by *E. faecium* MS79 (EPS-MS79) with Genbank accession number MF067509 isolated from low-water activity seafoods and characterized as potential probiotic by AlKalbani, Turner, & Ayyash (2019). Herein, we (i) isolated, purified and characterized EPS-MS79 including molecular weight, monosaccharide composition, potential structure by NMR analyses, functional groups by FTIR, particle size, zeta potential, and thermal properties by DSC; (ii) investigated bioactive properties of EPS-MS79 namely antioxidant by DPPH and ABTS, antidiabetic, antipathogenic, and anticancer activities, and (iii) investigated the rheological properties namely apparent viscosity, thermal behavior, viscoelastic properties, and thixotropic behavior as influenced by two salts ($CaCl_2$ and NaCl) and two pH levels (4.0 and 6.0)

2. Materials and Methods

All chemicals and reagents were purchased from Sigma-Aldrich (Chemie GmbH, Taufkirchen, Germany) unless otherwise stated.

2.1 Bacterial propagation

E. faecium MS79 (MF067509) stored in 50% glycerol solution at -80°C was activated in MRS broth (de Mann Rogosa Sharpe; LAB-M Limited, Lancashire, UK) at 37°C for 20 hours (h) and kept at 4°C. Two successive activations of *E. faecium* MS79 were performed prior to each EPS extraction step.

2.2 EPS extractions and purification

The extraction and purification of EPS produced by *E. faecium* MS79 (EPS-MS79) was based on previously reported methods (Nikolic et al., 2012). Briefly, *E. faecium* MS79 was cultivated in MRS broth (250 mL) supplemented with 20 g/L sucrose and incubated at 25°C for 48 h. The EPS-MS79 was purified by dialysis at 4°C for 48 h followed by lyophilization and freeze-dried. The purity of EPS solution (5 mg/mL) was confirmed by scanning for proteins and nucleic acid traces by UV-Vis spectrometer (Epoch™ 2, Bio-Tek, VT, USA) at 190-400 nm wavelength range. There was no absorbances at 260 nm and 280 nm indicating no or undetected proteins and nucleic acid traces.

2.3 EPS characterization

2.3.1 Determination of EPS-MS79 molecular weight

The EPS-MS79 Molecular weight (Mw) was determined by gel permeation chromatography (GPC) coupled with refractive index detector (Waters Cooperation, Herts, UK) as described by Kansandee, Moonmangmee, Moonmangmee, & Itsaranuwat (2019). Pullulan standard curve (Mw: 5 kDa, 10 kDa, 20 kDa, 50 kDa, 100 kDa) was used for calculation of Mw.

2.3.2 Monosaccharide composition

The purified EPS-MS79 was hydrolysed by 2 M trifluoroacetic acid (TFA) at 120°C for 2 h. Composition of monosaccharides was evaluated by GC-FID instrument (YL6500) coupled with HP-Ultra-2 column (25 m × 0.20 mm × 0.11 μm) as described by Wang et al. (2017b). The

monosaccharides which were used as standards are glucose, galactose, xylose, arabinose, fucose, and mannose.

2.3.3 FTIR spectroscopic study

Fourier transform-infrared **(**FTIR) analysis was carried out by attenuated total reflectance (ATR)-FTIR spectroscopy using Spectrum Two IR coupled with Universal ATR (UATR) unit (Perkin-Elmer Inc., Norwalk, CT, USA). Diamond/ZnSe crystal plate (Perkin-Elmer) was used for scanning purified-dried EPS-MS79 over a spectral range of 4000 cm^{-1} to 400 cm^{-1} at room temperature (23±0.1°C).

2.3.4 NMR analysis

The ^{1}H NMR, ^{13}C NMR, ^{1}H–^{13}C heteronuclear single quantum correlation (HSQC) spectra were recorded in D_2O using an Avance III Bruker 600 MHz spectrometer (Bruker Corporation, MA, USA) equipped with a cryo-probe according to the method described by Cheng et al. (2017). The EPS-MS79 structure was predicted by the online CASPER program (www.casper.organ.su.se/casper) (Jansson, Stenutz, & Widmalm, 2006) and performed as reported by (El-Deeb, Yassin, Al-Madboly, & El-Hawiet, 2018).

2.3.5 Thermal properties

The EPS-MS79 thermal behaviour was determined by the method described by Sasikumar, Kozhummal Vaikkath, Devendra, & Nampoothiri (2017). 25 mg purified EPS-MS79 was heated from 20°C to 350°C and analysed using a differential scanning calorimeter DSC 25 (TA instrument, DE, USA).

2.3.6 EPS microstructure study

A 5 mg of EPS-MS79 was used for microstructure study using JEOL JSM-6010LA scanning electron microscope (SEM, Akishima, Tokyo, Japan) operating at 20 kV accelerating voltage. A

thin gold layer was coated on EPS-MS79 using Cressington Sputter Coater 108 Auto (Ted Pella Inc., CA, USA).

2.3.7 Zeta potential and Particle size analysis

The particle size and zeta potential charge of EPS-MS79 (0.5% w/v) were measured using NanoPlus Zeta Potential & Particle Size Analyzer (Particulates System, GA, USA).

2.4 EPS bioactivities

2.4.1 Antioxidant by ABTS and DPPH assays

The free radical scavenging activities of EPS-MS79 (5 mg/mL or 10 mg/mL) were detected by 2,2′-azino-bis(3-ethylbenzo-thiazoline-6-sulphonic acid) ($ABTS^{\bullet+}$) and 1,1-diphenyl-2-picrylhydrazyl (DPPH) assays as reported by Ayyash, Al-Nuaimi, Al-Mahadin, & Liu (2018). The percentage of radical scavenging activity was expressed as scavenging (%) using:

$$\text{Scavenging } \% = \left(1 - \frac{Abs\ sample}{Abs\ blank}\right) \times\ 100 \ldots \text{Eq. (1)}$$

2.4.2 α-Amylase and α-glucosidase inhibitory activities

The EPS-MS79 (100 µg/mL or 200 µg/mL) inhibitory activities against α-amylase and α-glucosidase enzymes were measured by previously described method (Sasikumar et al., 2017).

$$\text{Inhibition } \% = \left(1 - \frac{Abs\ sample - Abs\ blank}{Abs\ control}\right) \times\ 100 \ldots \text{Eq. (2)}$$

2.4.3 Antiproliferative activity

The Antiproliferative activities of EPS-MS79 (5 mg/mL or 10 mg/mL) were evaluated in carcinoma cell lines Caco-2 (colon carcinoma) and MCF-7 (breast carcinoma). The assay was carried out according to the protocol described Ayyash et al. (2018). The percentage of cytotoxicity was calculated using:

$$\text{Antiproliferative } (\%) = \left[1 - \frac{\text{R}sample - Ro}{\text{R}ctrl - Ro}\right] \times\ 100 \ldots \text{Eq. (3)}$$

where Rsample and Rctrl represents ratio of absorbance (OD_{570}/OD_{605}) in the presence of EPS-MS79 and in the absence of EPS-MS79 [vehicle (positive) control] respectively. Ro [non-cell (negative) control] is the averaged background representing absorbance ratio of OD_{570}/OD_{605}.

2.4.4 Antipathogenic activity

The antipathogenic activities of EPS-MS79 (5 mg/mL) against foodborne pathogens *Staphylococcus aureus* ATCC 25923, *Salmonella* Typhimurium 02-8423, *Listeria monocytogenes* ATCC 7644, *E. coli* O157:H7 1934 were examined according to the previously described method (Jeong et al., 2017). EPS-MS79 aqueous (100 µL of 5 mg/mL) solution was added to 250 µL of the activated pathogen in brain heart infusion (BHI, LAB-M) followed by incubation at 37°C for 18 h. The pathogen was enumerated on BHI agar (LAB-M) and incubated at 37°C for 24 h in aerobic condition.

2.5 Rheological properties of EPS

EPS-MS79 was mixed (5 mg/mL) with different aqueous solutions (dd-H_2O, 0.1 M $CaCl_2$, 0.1 M NaCl) at pH values 4.0 and 6.0. Five rheological measurements were carried out for each EPS-MS79 solution using a Rheometer (Discovery Hybrid HR-2, TA Instruments, DE, USA). The geometry cone plate (50-mm diameter, 1° cone angle, 50 µm gap) with plate-controlled temperature (25°C ± 0.1°C) was employed to perform the following tests:

2.5.1 Apparent viscosity (η)

The shear rate ($\dot{\gamma}$) at 25°C ± 0.1°C was used to measure the shear stress (τ) and the apparent viscosity (η) of the samples. A shear rate range of 1000 s^{-1} to 10 s^{-1} was used to measure rheological property of the sample. All rheological tests were performed at 25°C ± 0.1°C. The increasing (forward measurements) and decreasing (backward measurements) shear rates were used to carry out the measurements. Thixotropy was measured as a function of the area between

the upward and downward curves using RHEOPLUS/32 V3.31 software. Power law model was employed to describe the flow curves of EPS-MS79:

$$\tau = m\dot{\gamma}^{n} \ldots \text{Eq. (4)}$$

where τ is shear stress (Pa), m is the consistency coefficient, $\dot{\gamma}$ is shear rate (s^{-1}), and n is the flow behaviour index.

2.5.2 Temperature-dependent behaviour

The change in viscosity of EPS-MS79 (η) was analyzed as a function of temperature from 10°C to 80°C. The temperature ramp rate was 3°C/min at a constant shear rate of 20 s^{-1}. Activation energy was calculated according to Arrhenius equation:

$$\eta = \eta_0 e^{\frac{E_a}{RT}} \ldots \text{Eq. (5)}$$

2.5.3 Amplitude and frequency sweep tests

Amplitude sweep was employed to determine the linear viscoelastic region of EPS-MS79 solutions in the strain range of (0.1 – 100%) and at a constant frequency of 1.0 Hz.

To evaluate viscoelastic behaviour of EPS-MS79 frequency sweep test was used at various frequencies ranging from 0.1 Hz to 10 Hz at constant strain within the linear viscoelastic region (less than 2%).

2.5.4 Thixotropy test

The solutions of EPS-MS79 were subjected to low and high shear to investigate the structural deterioration and recovery. The viscoelastic parameters storage (G') and loss (G") moduli were recorded using oscillation-time test at frequency 1.0 Hz. Three-time segments were applied with the following conditions: 1) first time (200 s, stress 0.2 Pa), 2) second time (60 s, stress 50 Pa), and third time (400 s, stress 0.2 Pa).

2.6 Statistical analysis

All biological activities were measured at least three times. Values were represented as the mean ± SD. One-way ANOVA was performed to determine the significance of differences between different concentrations. Fisher's test was carried out for comparing means at a significance level of $P < 0.05$.

3. Results and Discussion

3.1 Molecular weight and monosaccharides analysis

The average molecular weight (Mw) of the EPS-MS79 was determined by GPC method (Figure S1). Based on the external pullulan standard curve, the average Mw of the EPS-MS79 was 8.3 x 10^5 Da. This result is relatively larger than the Mw of EPS produced by *E. faecium* WEFA23 (2.5 – 3.23 x 10^5 Da) (Jia et al., 2019) and *E. faecium* MC13 (2.0 x 10^5 Da) (Kanmani et al., 2013). No Mw has been reported about EPS produced by *E. faecium* K1 (Bhat & Bajaj, 2018) and *E. faecium* BDU7 (Abdhul et al., 2014). The larger molecular weight contributes significantly to rheological properties and viscosity of the existence systems such food products (Zhou et al., 2019). As illustrated in Figure S2, the present EPS-MS79 composed of three monosaccharides arabinose, mannose, and glucose in a molar ratio of 0.8:1.7:11.3. This variation in monosaccharides suggests that EPS-MS79 was a hetero-exopolysaccharides. The monosaccharides type has significant influence on the functionalities of the exopolysaccharide (Zhou et al., 2019). The types of monosaccharides moieties of EPS-MS79 relatively differ compared with EPS produced by *E. faecium* WEFA23 (Jia et al., 2019) and *E. faecium* MC13 (Kanmani et al., 2013). Unlike the present study, both studies reported the presence of galactose and absence of arabinose moieties. This suggests that the present EPS-MS79 was a hetero-

exopolysaccharide and had distinctive monosaccharides composition compared with EPS produced by same bacterial species.

3.2 FTIR and NMR analyses

Functional group analysis by FTIR is presented in Figure 1. The peaks as appeared at 812.8 cm^{-1} and 915.65 cm^{-1} were ascribed to presence of α- and β-configurations of mono-sugars (Jeff et al., 2013). The peak absorption at 880.3 cm^{-1} implies the presence of β-glycosidic linkage. The peaks at 1027.1 cm-1 and 1127.4 cm^{-1} are the fingerprint peak of the polysaccharides. These peaks appeared due to stretch vibration of C-O-C and C-O-H linkages in the pyranose structure (Tian, Zhao, Zeng, Zhang, & Zheng, 2016). The band at 1213.8 cm^{-1} was assigned to presence of monosaccharide sugar in pyranose structure (Wang et al., 2017a). The peaks at 1545.4 cm^{-1} and 1645.8 cm^{-1} could be attributed to the vibration of C-O and C=O groups, respectively (Chen et al., 2013; Tian et al., 2016). The stretching vibration of C-H appeared as a peak signal at 2927.4 cm^{-1}. The wide band at 3285.3 cm^{-1} was accredited to large number of hydroxyl groups in the EPS-MS79 structure (Zeng et al., 2016). Functional groups have been linked with various EPS characteristics including viscosity, antimicrobial and antioxidant activities (Zhou et al., 2019). The FTIR spectrum of EPSs produced by *E. faecium* BDU7 (Abdhul et al., 2014) and *E. faecium* K1 (Bhat & Bajaj, 2018) are relatively different compared with the present EPS-MS79. This suggests that these exopolysaccharides have different characteristics. Jia et al. (2019) did not report FTIR spectrum of EPS produced by *E. faecium* WEFA23.

The NMR analyses including ^{1}H NRM, ^{13}C NMR, TOCSY, HSQC, and HMBC of EPS-MS79 are presented in Figure 2 (A, B, C, D and E, respectively). In addition to the 1D ^{1}H and ^{13}C traces

(Fig. 2A and 2B), the 2-D maps of TOCSY and HSQC (Fig. 2C and 2D) illustrate the anomeric proton and carbon correlations that typically occur in the regions 4.5 - 5.5 ppm (^{1}H) and 95.0 - 110.0 ppm (^{13}C). Panel E of Figure 2 shows the HMBC map that confirms the expected pattern for the long-range connections in the polysaccharide regions. The presence of uronate or acetyl-uronate derivatives, that could be possible in principle because of the occurrence of a weak broadened signal in the carbonyl ^{13}C region, is not ruled out by the HMBC spectrum (Fig. 2E). The observation of a weak HSQC correlation linking a carbon at 72.6 ppm to a proton at 4.62 ppm, accompanied by a weaker one at 76.8 and 5.37 ppm (Fig 2C), seems to support the interpretation in favor of an uronate derivative in EPS-MS79, in either α and β anomeric configuration (Ma et al., 2018; Ye, Chen, Wang, Yang, & Bin, 2018). The CASPER computed assignments (Lundborg & Widmalm, 2011) of the experimental anomeric CH correlations obtained from ^{1}H-^{13}C NMR HQSC are presented in Table 1. According to the CASPER outcomes, the proposed backbone structure of EPS-MS79 was: →4)[α-d-Gal(1→4)α-d-Glc(1→3)α-d-Glc(1→2)]β-d-Man(1→2)α-d-Glc(1→6)α-d-Glc(1→. To best of our knowledge, no information has been reported about the potential backbone structure of EPS produced by *E. faecium* strains (Abdhul et al., 2014; Bhat & Bajaj, 2018; Jia et al., 2019).

3.3 Thermal properties, particle size, zeta potential and SEM

The thermodynamic analysis by DSC demonstrated that the transition temperature (T_g) of EPS-MS79 was detected at 58.6°C followed by sharp peak indicated for melting temperature at 161.0°C (Fig. 3A). The enthalpy energy at the T_m was 195.7 J/g. The present T_m of EPS-MS79 is greater than EPS produced by *E. faecium* K1 (T_m 62.99°C) (Bhat & Bajaj, 2018) and *E. faecium*

MC13 (T_m 125.89°C) (Kanmani et al., 2013). EPS with higher T_m has great application in the industrial processes which require thermal treatments such food production (Xu et al., 2019). The particle size analyzer found that the average molecular size and the zeta potential of the EPS-MS79 were 561.7 nm and -109.97 mV, respectively. The size and charge of the EPS-MS79 are comparable to those reported of EPS produced by *Pediococcus pentosaceus* M41(Ayyash et al., 2020b). It has been reported that negative charge usually associated with noticeable bioactive properties of EPS (Xu et al., 2019). The negative charge of the EPS-MS79 may be due to hydroxyl and carboxyl groups composed the EPS structure. SEM images at 2000x (Fig. 3B) and 800x (Fig. 3C) magnifications of the EPS-MS79 demonstrated a layer-like, flake-like and closed structure. The presence of 1→4 and 1→3 linkages may be responsible for the layer-like structure which in turn provides firm structural properties (Zhou et al., 2019).

3.4 Bioactive properties

3.4.1 Antioxidant, Antidiabetic and Antiproliferative Activities

The results of the bioactive properties namely antioxidant measured by DPPH and ABTS, antidiabetic measured α-amylase and α-glucosidase inhibitions activities, antiproliferative activity against colon (Caco-2) and breast (MCF-7) carcinoma cell lines, and antibacterial activities against 4 foodborne pathogens are presented in Figure 4. Free radicals (superoxide ($^{\bullet}O_2^-$, $^{\bullet}$OOH), hydroxyl ($^{\bullet}$OH), and peroxyl (ROO$^{\bullet}$)) cause pronounced stress and damage to cell components (Saadat et al., 2019). The antioxidant activity of the bacterial EPS is a major bioactive parameter frequently assessed by enormous studies related to EPS. Scavenging activities of EPS-MS79 were 76% and 85% as measured by DPPH and 26% and 44% as measured by ABTS at 5 mg and 10 mg concentrations, respectively (Fig. 4A). The current DPPH

results are comparable to the DPPH activities of EPS produced by *E. faecium* K1 (64%) (Bhat & Bajaj, 2018) and greater than *E. faecium* BDU7 (Abdhul et al., 2014). Functional groups (hydroxyl and carboxyl), monosaccharide composition, and substitutions of EPS are main determinants of the antioxidant activities (Zhou et al., 2019). Statistical analysis displayed that EPS-MS79 concentration affected the antioxidant activities significantly ($p < 0.05$) (Fig. 4A). Inhibiting the activities of α-amylase and α-glucosidase is one of the approaches to protect diabetic people by blocking carbohydrates hydrolysis by these enzymes (Ayyash et al., 2019). EPS-MS79 exhibited remarkable inhibitions activities against α-amylase (87% and 91%) and α-glucosidase (91% an 92%) at 100 µg and 200 µg concentrations, respectively (Fig. 4A). To best of our knowledge, no information has been reported previously about the antidiabetic activities of EPS produced by *E. faecium* (Abdhul et al., 2014; Bhat & Bajaj, 2018; Kanmani et al., 2013). However, the present results are comparable to those found by Ayyash et al. (2020b) and Sasikumar et al. (2017) who reported antidiabetic properties of EPS produced by *Pediococcus pentosaceus* M41 and *L. plantarum* BR2, respectively. To present, the inhibition mechanism of the α-amylase and α-glucosidase activities is unclear. For instance, α-amylase activity could be inhibited by either blocking the active site, altering the allosteric site of the enzyme, or attaching to the enzyme's substrate which by then would be unavailable to be hydrolyzed by the enzyme (Aghajari, Feller, Gerday, & Haser, 2002; Tundis, Loizzo, & Menichini, 2010). According to statistical analysis, there was no significant effect ($p > 0.05$) of EPS-MS79 concentration on the inhibition activities of α-amylase and α-glucosidase.

As can be depicted from Figure 4A, EPS-MS79 displayed antiproliferative activities against colon (72% and 77%) and breast (43% and 56%) cancer cell lines at 5 mg and 10 mg

concentrations, respectively. The antiproliferative magnitude of EPS-MS79 on colon cancer (Caco-2) was greater ($p < 0.05$) compared with breast cancer (MCF-7). Like the antidiabetic, there are no anticancer activities have been reported about EPS produced by *E. faecium*. However, our results accord with the anticancer activities of EPS produced by *R. mucilaginosa* CICC 33013 (Ma et al., 2018) and are greater than EPS of *L. plantarum* C70 (Ayyash et al., 2020a). Several hypotheses have been proposed to explain the anticancer mechanism(s) of EPS (Saadat et al., 2019). EPS could induce the autophagy via regulating the autophagy Beclin-I protein (Kim, Oh, Yun, Oh, & Kim, 2010). EPS could also block the cancer cell receptors which in turn prevent growth promotors to enter the cells (De Flora & Ferguson, 2005).

3.4.2 Antibacterial Activities

Figure 4B displays the antibacterial activities of EPS-MS79 against 4 foodborne pathogens namely *S. aureus*, *S.* Typhimurium, *L. monocytogenes*, and *E. coli* O157:H7. The EPS-MS79 had significant ($p < 0.05$) bactericide impact on all experimented foodborne pathogens. The reductions in the pathogens' population were 2.7, 3.0, 3.0 and 2.9 logs CFU/mL for *S. aureus*, *S.* Typhimurium, *L. monocytogenes*, and *E. coli* O157:H7, respectively, compared with the initial 9.1 – 9.2 logs CFU/mL (Fig. 4B). There was no significant difference between the log reductions of the pathogens. This suggests that EPS-MS79 had similar bactericidal effects on both gram-positive and gram-negative pathogens. The mechanism(s) of the antibacterial effect of the EPS is yet unclear. However, few hypotheses have been proposed in literatures explaining the antimicrobial mechanisms of the EPS. It has been reported that EPS could block the enzymes responsible for the cell wall biosynthesis which leads to leakage in cell components followed by cell death (Vazquez-Rodriguez et al., 2018). We also propose that EPS might lead to cell

starvation by preventing nutrients entrance via blocking cell-wall porins. This proposal requires further investigations.

3.5 Rheological behaviors

Rheological properties are the foremost features attract various industries' attention to EPS. The capabilities of EPS to flow, bind water (water-holding), form a gel, and maintain original characteristics under various industrial processes are crucial for, but not limited, food, pharmaceutical and packaging industries. Furthermore, the EPS stability under various temperatures, salt type and pH level are highly regarded. The experimented EPS-MS79 was subjected to different rheological tests with presence of NaCl (anion) and $CaCl_2$ (cation) at two pH values 4.0 and 6.0. To the best of our knowledge, no rheological information is available about EPS produced by *E. faecium*.

3.5.1 Apparent viscosity (η) and temperature-dependent behavior

All EPS-MS79 solutions displayed shear thinning behavior, as η decreased along with shear rate increase, regardless of the salt type and pH level (Fig. 5A). As can depicted from Fig. 5A, EPS-MS79 solution in presence and absence of $CaCl_2$ at pH 4.0 showed highest and lowest, respectively, apparent viscosity at shear rate $\leq 80\ s^{-1}$. However, the presence of $CaCl_2$ at pH 6.0 exhibited lower η. These results suggest an interaction effect of $CaCl_2$ and pH at level 4.0 on the η. The η results fitted well with Power law model. The highest deviation from the Newtonian behavior (n = 1.00) was scored by EPS-MS79 solution with $CaCl_2$ at pH 4.0 (n = 0.54) (Table S). the competence of the cations and anions to build intermolecular bridges within the EPS structure has been reported (Li et al., 2017). However, the present study reveals that pH level had noticeable and positive impact on the cation bridging capacity. This finding disagrees with (Li et

al., 2017) who reported higher viscosity of EPS-POS16 at pH 6.0 to 9.0; however, authors did not investigate the cations impact at different pH level. On the other hand, Ahmed, Wang, Anjum, Ahmad, & Khan (2013) have found that the viscosity of ESP-ZW3 decreased at neutral pH. In this study, we postulate that the lower pH 4.0 may affect the EPS conformation which improved the capacity of Ca^{+2} to form intermolecular bridges. The highest η in this study contradict with the results reported by (Ayyash et al., 2020b). This contradiction may be due to differences in EPS composition and structure.

Fig. 5B presents the viscosity behavior of all EPS-MS79 solutions functioned to temperature elevation. After 22°C, all EPS-MS79 solutions had similar viscosity till 350°C. This result implies that the thermal energy after 22°C was enough to break down the polymer structure. This finding suggests that the present EPS-MS79 is not suitable for high thermal processes. The highest activation energy calculated according to Arrhenius equation was EPS-MS79 prepared with $CaCl_2$ at pH 4.0. This result concurs with apparent viscosity of the same solution (Fig. 5A). The thermal behavior of the EPS-MS79 in presence of $CaCl_2$ at pH 4.0 supports the concept of the intermolecular bridging by Ca^{+2}. Comparatively, the thermal stability of the EPS-MS79 is less than EPS produced by *P. pentosaceus* M41 (Ayyash et al., 2020b). This difference could be attributed to the variation in EPS composition and structural linkage.

3.5.2 Storage (G`) and Loss (G``) moduli

The amplitude sweep test showed that all EPS-MS79 solutions maintained a linear behavior for storage (G') and loss (G") over a strain range between 0.01 to 5.0% (Fig. 6A and 6B). The G' (elastic) was greater than G" (viscus). This result is different than the result reported by Ayyash et al. (2020b) who reported that G" was greater than G' of EPS-M41 and linear behavior up to 2%

411 strain only. Our result also contradicts with result reported by Han, Du, Xu, Qian, & Zhang
412 (2016).
413 The G' and G" moduli as functioned to frequency range from 0.1 to 20 Hz of the EPS-MS79
414 solutions prepared with different salt types and pH values are displayed in Figures 7A and 7B,
415 respectively. Both moduli of all EPS-MS79 solutions increased alongside with frequency
416 increase. In agreement with apparent viscosity results, the G' (Fig. 7A) and G" (Fig. 7B) of the
417 EPS-MS79 solution with $CaCl_2$ at pH 4.0 were the highest; whereas, the EPS-MS79 with water
418 only at pH 4.0 had the lowest G' and G". This result evident the intermolecular bridging may
419 occur by aid of Ca^{+2}. The impact of salt on EPS viscosity is a controversial concept. Andhare et
420 al. (2017) did not report a noticeable impact of anions (Na^{+1}, K^{+1}) and cations (Mg^{+2} and Ca^{+2}) on
421 viscosity of EPS produced by *Rhizobium radiobacter* CAS. On the other hand, a reduction in the
422 viscoelastic properties of EPS produced by *Rhizobium* because of NaCl has been reported by
423 Aranda-Selverio et al. (2010). It is well stated that the viscoelastic behavior of the EPS is highly
424 influenced by the following factors: Mw, monosaccharide composition, type of glycosidic bond,
425 substitutions and functional groups (Zhou et al., 2019). Therefore, the salt and pH impact would
426 be influenced by the same aforementioned factors. Figure 7C demonstrates that that the viscous
427 modulus is greater than storage modulus for all EPS-MS79 solutions at low frequency (tan delta
428 (δ) > 1.0). The δ decrease with frequency increase allowed for the elastic behavior to be
429 dominant at high frequency.
430 **3.5.3 Thixotropic behavior (Time-dependent test)**
431 Some products, especially foods, are subjected to high shear stress during processing and
432 transportation. This high shear stress creates major defect in the structure of the final products
433 which become undesirable to end consumers. EPS could play crucial role to alleviate this

phenomenon. EPS capable to re-build its original structure after the EPS undergo for magnitude shear stress. This capability varies between different EPSs based on the Mw, monosaccharide composition, type of glycosidic bond, substitutions and functional groups. As can be depicted from Figure 8, thixotropic behaviors were detected for EPS-MS79 solutions prepared with $CaCl_2$ at pH 4.0 and NaCl at pH 6.0. Whereas, EPS-MS79 with NaCl at pH 4.0 demonstrated an anti-thixotropic behavior. These results suggest that salt type and pH level are determinants affecting the thixotropic behavior. This result disagrees with those reported by Ayyash et al. (2020b) who found that the thixotropic behavior did not respond to presence of anion (Na^{+1}) or cation (Ca^{+2}). This disagreement may be attributed to the differences in EPS composition, linkages, and functional groups.

4. Conclusions

EPSs are valuable biopolymers to various industrial sections especially food and pharmaceutical sectors. EPS-MS79 had relatively large molecular weight that preferred by industries. EPS-MS79 exhibited pronounced bioactive properties make it a potent ingredient in various food formula as prebiotic. All EPS-MS79 exhibited a non-Newtonian behavior (shear-thinning) The rheological properties were affected by the presence of salts and pH level.

Acknowledgement

The authors are thankful to Mr. Mustapha Mby, Dr. Hassan Abdallah, Dr. Fatullah Hamed, and Dr. Jaleel Kizhakkayil from UAEU for technical support.

Funding

This study was funded by the United Arab Emirates University (UAEU) via the UPAR project grant code G00003248 (31F135).

Author Contributions

Mutamed Ayyash: Conceptualization, Supervision, Visualization & Writing - Original Draft; **Constantinos Stathopoulos & Mohammad Baig**: Writing - Original Draft; **Basim Abu-Jdayil**: Conceptualization, Visualization & Writing - Original Draft; **Gennaro Esposito**: Formal analysis; **Mark Turner & Ahmad Baba & Vasso Apostolopoulos**: Conceptualization and Writing - Review & Editing; **Anas Al-Nabulsi & Tareq Osaili**: Validation and Writing - Review & Editing

5. References

Abdhul, K., Ganesh, M., Shanmughapriya, S., Kanagavel, M., Anbarasu, K., & Natarajaseenivasan, K. (2014). Antioxidant activity of exopolysaccharide from probiotic strain enterococcus faecium (bdu7) from ngari. *International Journal of Biological Macromolecules, 70*, 450-454. doi:10.1016/j.ijbiomac.2014.07.026

Aghajari, N., Feller, G., Gerday, C., & Haser, R. (2002). Structural basis of α-amylase activation by chloride. *Protein Science, 11*(6), 1435-1441. doi:10.1110/ps.0202602

Ahmed, Z., Wang, Y., Anjum, N., Ahmad, A., & Khan, S. T. (2013). Characterization of exopolysaccharide produced by lactobacillus kefiranofaciens zw3 isolated from tibet kefir – part ii. *Food Hydrocolloids, 30*(1), 343-350. doi:10.1016/j.foodhyd.2012.06.009

AlKalbani, N. S., Turner, M. S., & Ayyash, M. M. (2019). Isolation, identification, and potential probiotic characterization of isolated lactic acid bacteria and in vitro investigation of the cytotoxicity, antioxidant, and antidiabetic activities in fermented sausage. *Microbial Cell Factories, 18*(1), 188. doi:10.1186/s12934-019-1239-1

Aranda-Selverio, G., Penna, A. L. B., Campos-Sás, L. F., Santos Junior, O. d., Vasconcelos, A. F. D., Silva, M. d. L. C. d., Lemos, E. G. M., Campanharo, J. C., & Silveira, J. L. M. (2010). Propriedades reológicas e efeito da adição de sal na viscosidade de exopolissacarídeos produzidos por bactérias do gênero rhizobium. *Química Nova*, 895-899.

Ayyash, M., Abu-Jdayil, B., Itsaranuwat, P., Galiwango, E., Tamiello-Rosa, C., Abdullah, H., Esposito, G., Hunashal, Y., Obaid, R. S., & Hamed, F. (2020a). Characterization, bioactivities, and rheological properties of exopolysaccharide produced by novel probiotic lactobacillus plantarum c70 isolated from camel milk. *International Journal of Biological Macromolecules*.

Ayyash, M., Abu-Jdayil, B., Olaimat, A., Esposito, G., Itsaranuwat, P., Osaili, T., Obaid, R., Kizhakkayil, J., & Liu, S.-Q. (2020b). Physicochemical, bioactive and rheological properties of an exopolysaccharide produced by a probiotic pediococcus pentosaceus m41. *Carbohydrate Polymers*, 115462.

Ayyash, M., Al-Nuaimi, A. K., Al-Mahadin, S., & Liu, S.-Q. (2018). In vitro investigation of anticancer and ace-inhibiting activity, α-amylase and α-glucosidase inhibition, and antioxidant activity of camel milk fermented with camel milk probiotic: A comparative study with fermented bovine milk. *Food Chemistry*, *239*, 588-597.

Ayyash, M., Johnson, S. K., Liu, S.-Q., Mesmari, N., Dahmani, S., Al Dhaheri, A. S., & Kizhakkayil, J. (2019). In vitro investigation of bioactivities of solid-state fermented lupin, quinoa and wheat using lactobacillus spp. *Food Chemistry*, *275*, 50-58. doi:10.1016/j.foodchem.2018.09.031

Bhat, B., & Bajaj, B. K. (2018). Hypocholesterolemic and bioactive potential of exopolysaccharide from a probiotic enterococcus faecium k1 isolated from kalarei. *Bioresource Technology*, *254*, 264-267. doi:10.1016/j.biortech.2018.01.078

Caggianiello, G., Kleerebezem, M., & Spano, G. (2016). Exopolysaccharides produced by lactic acid bacteria: From health-promoting benefits to stress tolerance mechanisms. *Applied Microbiology and Biotechnology*, *100*(9), 3877-3886. doi:10.1007/s00253-016-7471-2

505 Chen, Y., Mao, W., Wang, J., Zhu, W., Zhao, C., Li, N., Wang, C., Yan, M., Guo, T., & Liu, X. (2013).
506 Preparation and structural elucidation of a glucomannogalactan from marine fungus penicillium
507 commune. *Carbohydrate Polymers, 97*(2), 293-299. doi:10.1016/j.carbpol.2013.05.004
508 Cheng, Y., Xiao, X., Li, X., Song, D., Lu, Z., Wang, F., & Wang, Y. (2017). Characterization, antioxidant
509 property and cytoprotection of exopolysaccharide-capped elemental selenium particles
510 synthesized by bacillus paralicheniformis sr14. *Carbohydrate Polymers, 178*, 18-26.
511 doi:10.1016/j.carbpol.2017.08.124
512 De Flora, S., & Ferguson, L. R. (2005). Overview of mechanisms of cancer chemopreventive agents.
513 *Mutation Research/Fundamental and Molecular Mechanisms of Mutagenesis, 591*(1-2), 8-15.
514 doi:10.1016/j.mrfmmm.2005.02.029
515 El-Deeb, N. M., Yassin, A. M., Al-Madboly, L. A., & El-Hawiet, A. (2018). A novel purified lactobacillus
516 acidophilus 20079 exopolysaccharide, la-eps-20079, molecularly regulates both apoptotic and nf-
517 kappab inflammatory pathways in human colon cancer. *Microbial Cell Factories, 17*(1), 29.
518 doi:10.1186/s12934-018-0877-z
519 Han, M., Du, C., Xu, Z. Y., Qian, H., & Zhang, W. G. (2016). Rheological properties of phosphorylated
520 exopolysaccharide produced by sporidiobolus pararoseus jd-2. *International Journal of Biological*
521 *Macromolecules, 88*, 603-613. doi:10.1016/j.ijbiomac.2016.04.035
522 Hussain, A., Zia, K. M., Tabasum, S., Noreen, A., Ali, M., Iqbal, R., & Zuber, M. (2017). Blends and
523 composites of exopolysaccharides; properties and applications: A review. *International Journal of*
524 *Biological Macromolecules, 94*(Pt A), 10-27. doi:10.1016/j.ijbiomac.2016.09.104
525 Jansson, P.-E., Stenutz, R., & Widmalm, G. (2006). Sequence determination of oligosaccharides and
526 regular polysaccharides using nmr spectroscopy and a novel web-based version of the computer
527 program casper. *Carbohydrate Research, 341*(8), 1003-1010.
528 Jeff, I. B., Li, S., Peng, X., Kassim, R. M., Liu, B., & Zhou, Y. (2013). Purification, structural elucidation
529 and antitumor activity of a novel mannogalactoglucan from the fruiting bodies of lentinus edodes.
530 *Fitoterapia, 84*, 338-346. doi:10.1016/j.fitote.2012.12.008

Jeong, D., Kim, D.-H., Kang, I.-B., Kim, H., Song, K.-Y., Kim, H.-S., & Seo, K.-H. (2017). Characterization and antibacterial activity of a novel exopolysaccharide produced by lactobacillus kefiranofaciens dn1 isolated from kefir. *Food Control, 78*, 436-442. doi:10.1016/j.foodcont.2017.02.033

Jia, K., Tao, X., Liu, Z., Zhan, H., He, W., Zhang, Z., Zeng, Z., & Wei, H. (2019). Characterization of novel exopolysaccharide of enterococcus faecium wefa23 from infant and demonstration of its in vitro biological properties. *International Journal of Biological Macromolecules, 128*, 710-717. doi:10.1016/j.ijbiomac.2018.12.245

Jiang, Y., & Yang, Z. (2018). A functional and genetic overview of exopolysaccharides produced by lactobacillus plantarum. *Journal of Functional Foods, 47,* 229-240. doi:10.1016/j.jff.2018.05.060

Kanmani, P., Suganya, K., Satish kumar, R., Yuvaraj, N., Pattukumar, V., Paari, K. A., & Arul, V. (2013). Synthesis and functional characterization of antibiofilm exopolysaccharide produced by enterococcus faecium mc13 isolated from the gut of fish. *Applied Biochemistry and Biotechnology, 169*(3), 1001-1015. doi:10.1007/s12010-012-0074-1

Kansandee, W., Moonmangmee, D., Moonmangmee, S., & Itsaranuwat, P. (2019). Characterization and bifidobacterium sp. Growth stimulation of exopolysaccharide produced by enterococcus faecalis ejrm152 isolated from human breast milk. *Carbohydrate Polymers, 206*, 102-109. doi:10.1016/j.carbpol.2018.10.117

Kim, Y., Oh, S., Yun, H., Oh, S., & Kim, S. (2010). Cell-bound exopolysaccharide from probiotic bacteria induces autophagic cell death of tumour cells. *Letters in Applied Microbiology, 51*(2), 123-130. doi:10.1111/j.1472-765X.2010.02859.x

Kimmel, S. A., Roberts, R. F., & Ziegler, G. R. (1998). Optimization of exopolysaccharide production by lactobacillus delbrueckii subsp. Bulgaricus rr grown in a semidefined medium. *Applied and Environmental Microbiology, 64*(2), 659-664.

Li, J., Xu, H., Chen, X., Xu, L., Cheng, R., Zhang, J., & Wang, S. (2017). Characterization of an exopolysaccharide with distinct rheological properties from paenibacillus edaphicus nust16.

International Journal of Biological Macromolecules, 105(Pt 1), 1-8. doi:10.1016/j.ijbiomac.2017.06.030

Llamas-Arriba, M. G., Peirotén, Á., Puertas, A. I., Prieto, A., López, P., Pardo, M. Á., Rodríguez, E., & Dueñas, M. T. (2019). Heteropolysaccharide-producing bifidobacteria for the development of functional dairy products. *LWT, 102*, 295-303. doi:10.1016/j.lwt.2018.12.044

Lundborg, M., & Widmalm, G. r. (2011). Structural analysis of glycans by nmr chemical shift prediction. *Analytical Chemistry, 83*(5), 1514-1517. doi:10.1021/ac1032534

Ma, W., Chen, X., Wang, B., Lou, W., Chen, X., Hua, J., Sun, Y. J., Zhao, Y., & Peng, T. (2018). Characterization, antioxidativity, and anti-carcinoma activity of exopolysaccharide extract from rhodotorula mucilaginosa cicc 33013. *Carbohydrate Polymers, 181*, 768-777. doi:10.1016/j.carbpol.2017.11.080

Monsan, P., Bozonnet, S., Albenne, C., Joucla, G., Willemot, R.-M., & Remaud-Siméon, M. (2001). Homopolysaccharides from lactic acid bacteria. *International Dairy Journal, 11*(9), 675-685. doi:Doi 10.1016/S0958-6946(01)00113-3

Nicolaus, B., Kambourova, M., & Oner, E. T. (2010). Exopolysaccharides from extremophiles: From fundamentals to biotechnology. *Environmental Technology, 31*(10), 1145-1158. doi:10.1080/09593330903552094

Nikolic, M., López, P., Strahinic, I., Suárez, A., Kojic, M., Fernández-García, M., Topisirovic, L., Golic, N., & Ruas-Madiedo, P. (2012). Characterisation of the exopolysaccharide (eps)-producing lactobacillus paraplantarum bgcg11 and its non-eps producing derivative strains as potential probiotics. *International Journal of Food Microbiology, 158*(2), 155-162. doi:10.1016/j.ijfoodmicro.2012.07.015

Roberts, C. M., Fett, W. F., Osman, S. F., Wijey, C., O'Connor, J. V., & Hoover, D. G. (1995). Exopolysaccharide production by bifidobacterium longum bb-79. *Journal of Applied Bacteriology, 78*(5), 463-468. doi:10.1111/j.1365-2672.1995.tb03085.x

Ryan, K. J., & Ray, C. G. (2004). Medical microbiology. *McGraw Hill, 4*, 370.

583 Saadat, R. Y., Khosroushahi, Y. A., & Gargari, P. B. (2019). A comprehensive review of anticancer,
584 immunomodulatory and health beneficial effects of the lactic acid bacteria exopolysaccharides.
585 *Carbohydrate Polymers, 217*, 79-89. doi:10.1016/j.carbpol.2019.04.025
586 Sasikumar, K., Kozhummal Vaikkath, D., Devendra, L., & Nampoothiri, K. M. (2017). An
587 exopolysaccharide (eps) from a lactobacillus plantarum br2 with potential benefits for making
588 functional foods. *Bioresource Technology, 241*, 1152-1156. doi:10.1016/j.biortech.2017.05.075
589 Silva, L. A., Lopes Neto, J. H. P., & Cardarelli, H. R. (2019). Exopolysaccharides produced by
590 lactobacillus plantarum: Technological properties, biological activity, and potential application in
591 the food industry. *Annals of Microbiology, 69*(4), 321-328. doi:10.1007/s13213-019-01456-9
592 Tian, Y., Zhao, Y., Zeng, H., Zhang, Y., & Zheng, B. (2016). Structural characterization of a novel neutral
593 polysaccharide from lentinus giganteus and its antitumor activity through inducing apoptosis.
594 *Carbohydrate Polymers, 154*, 231-240. doi:10.1016/j.carbpol.2016.08.059
595 Tundis, R., Loizzo, M., & Menichini, F. (2010). Natural products as α-amylase and α-glucosidase
596 inhibitors and their hypoglycaemic potential in the treatment of diabetes: An update. *Mini Reviews*
597 *in Medicinal Chemistry, 10*(4), 315-331.
598 Vazquez-Rodriguez, A., Vasto-Anzaldo, X. G., Perez, D. B., Vázquez-Garza, E., Chapoy-Villanueva, H.,
599 García-Rivas, G., Garza-Cervantes, J. A., Gómez-Lugo, J. J., Gomez-Loredo, A. E., & Gonzalez,
600 M. T. G. (2018). Microbial competition of rhodotorula mucilaginosa uanl-001l and e. Coli
601 increase biosynthesis of non-toxic exopolysaccharide with applications as a wide-spectrum
602 antimicrobial. *Scientific Reports, 8*(1), 798. doi:ARTN 798

603 10.1038/s41598-017-17908-8

604 Wang, X., Shao, C., Liu, L., Guo, X., Xu, Y., & Lü, X. (2017a). Optimization, partial characterization and
605 antioxidant activity of an exopolysaccharide from lactobacillus plantarum kx041. *International*
606 *Journal of Biological Macromolecules, 103*, 1173-1184. doi:10.1016/j.ijbiomac.2017.05.118

Wang, X., Zhang, L., Wu, J., Xu, W., Wang, X., & Lu, X. (2017b). Improvement of simultaneous determination of neutral monosaccharides and uronic acids by gas chromatography. *Food Chemistry*, *220*, 198-207. doi:10.1016/j.foodchem.2016.10.008

Xu, Y., Cui, Y., Yue, F., Liu, L., Shan, Y., Liu, B., Zhou, Y., & Lü, X. (2019). Exopolysaccharides produced by lactic acid bacteria and bifidobacteria: Structures, physiochemical functions and applications in the food industry. *Food Hydrocolloids*, *94*, 475-499. doi:10.1016/j.foodhyd.2019.03.032

Ye, G., Chen, Y., Wang, C., Yang, R., & Bin, X. (2018). Purification and characterization of exopolysaccharide produced by weissella cibaria yb-1 from pickle chinese cabbage. *International Journal of Biological Macromolecules*, *120*(Pt A), 1315-1321. doi:10.1016/j.ijbiomac.2018.09.019

Zeng, H., Miao, S., Zhang, Y., Lin, S., Jian, Y., Tian, Y., & Zheng, B. (2016). Isolation, preliminary structural characterization and hypolipidemic effect of polysaccharide fractions from fortunella margarita (lour.) swingle. *Food Hydrocolloids*, *52*, 126-136. doi:10.1016/j.foodhyd.2015.05.028

Zhou, Y., Cui, Y., & Qu, X. (2019). Exopolysaccharides of lactic acid bacteria: Structure, bioactivity and associations: A review. *Carbohydrate Polymers*, *207*, 317-332. doi:10.1016/j.carbpol.2018.11.093

Table 1: The ^{1}H and ^{13}C chemical shifts assignments of EPS-MS79

Residues	Chemical shifts (ppm)[1]					
	1	2	3	4	5	6,6’
→6)α-d-Glc^{i}(1→	103.26	74.24	74.70	69.57	72.77	65.19
	5.30	3.33	3.83	4.02	4.64	4.80,5.34
→2)α-d-Glc^{ii}(1→	105.69	80.99	73.02	70.56	73.21	61.59
	5.08	3.96	4.89	4.10	3.83	4.56,5.09
→2,4)β-d-Man^{iii}(1→	102.09	79.73	75.23	75.90	76.68	63.78
	5.22	5.00	4.98	4.50	3.63	5.23,5.20
→3)α-d-Glc^{iv}(1→	105.29	72.41	81.38	70.55	72.51	61.28
	5.11	3.70	4.39	3.69	4.52	4.76,4.86
→4)α-d-Glc^{v}(1→	100.92	72.36	76.55	77.99	72.65	61.40
	5.36	3.69	4.95	3.77	4.76	5.43,5.12
α-d-Gal^{vi}(1→	104.90	68.22	69.40	69.10	72.74	61.79
	5.37	5.03	5.23	5.17	4.76	4.36,4.25

[1] the chemical shifts assignment by CASPER software (Lundborg & Widmalm, 2011).

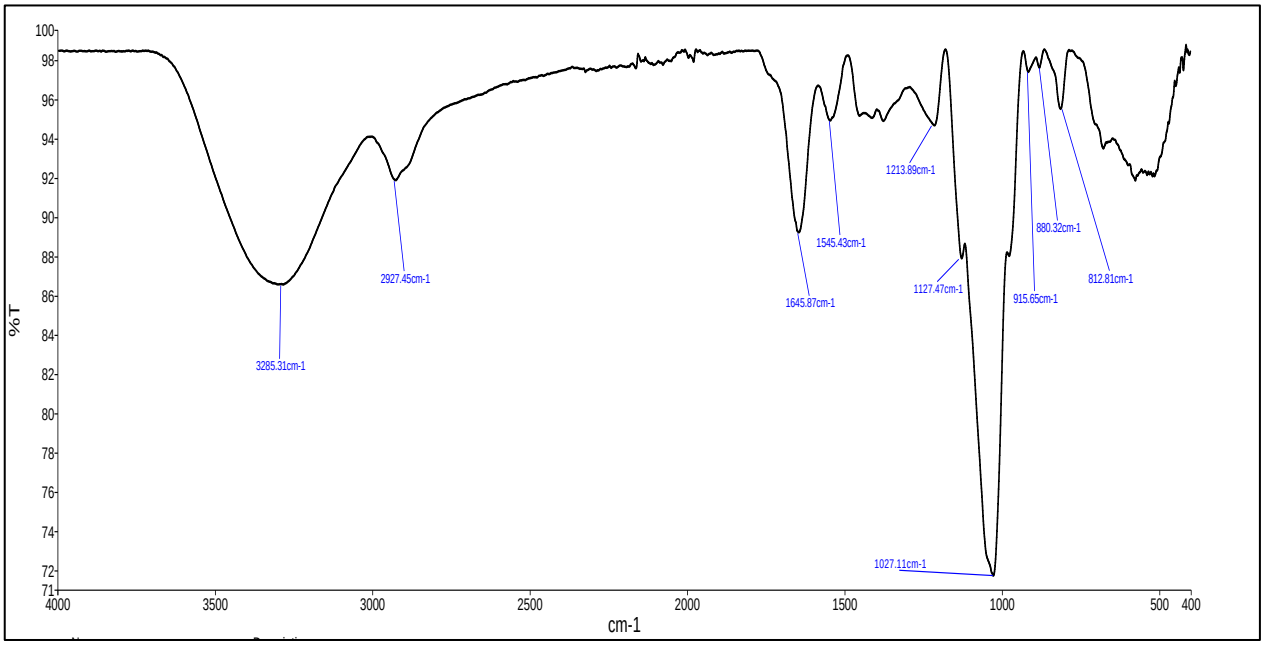

Figure 1: ATR-FTIR spectrum of the EPS-MS79

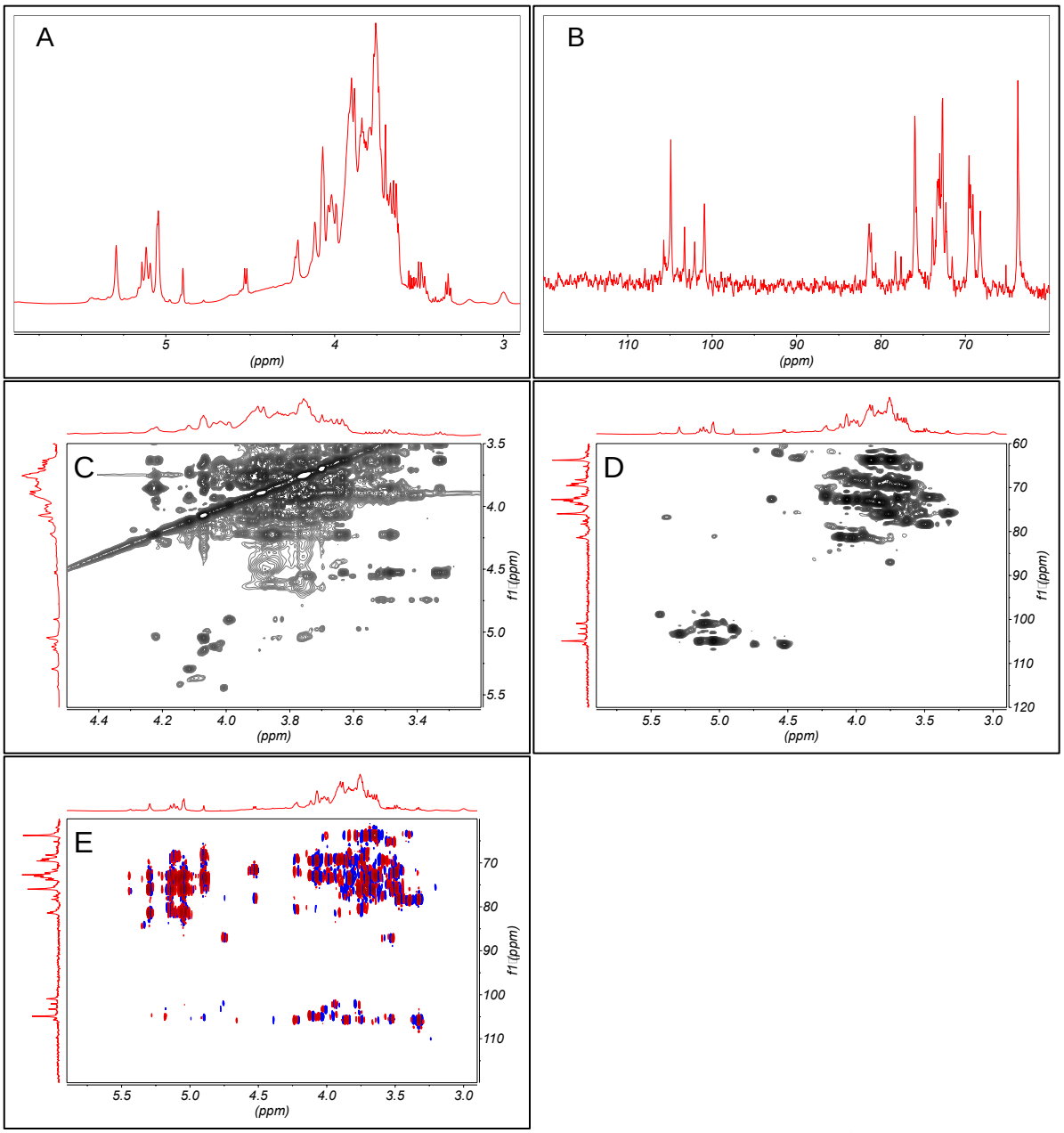

Figure 2: One- and two-dimensional NMR spectra of EPS-MS79 (A) 1D ^{1}H spectrum, (B) 1D ^{13}C spectrum, (C) 2D ^{1}H TOCSY, (D) 2D ^{13}C-^{1}H HSQC spectrum, (E) 2D ^{13}C-^{1}H HSQC. black contours: 2D ^{13}C-^{1}H HSQC, red-blue contours: 2D ^{13}C-^{1}H HMBC

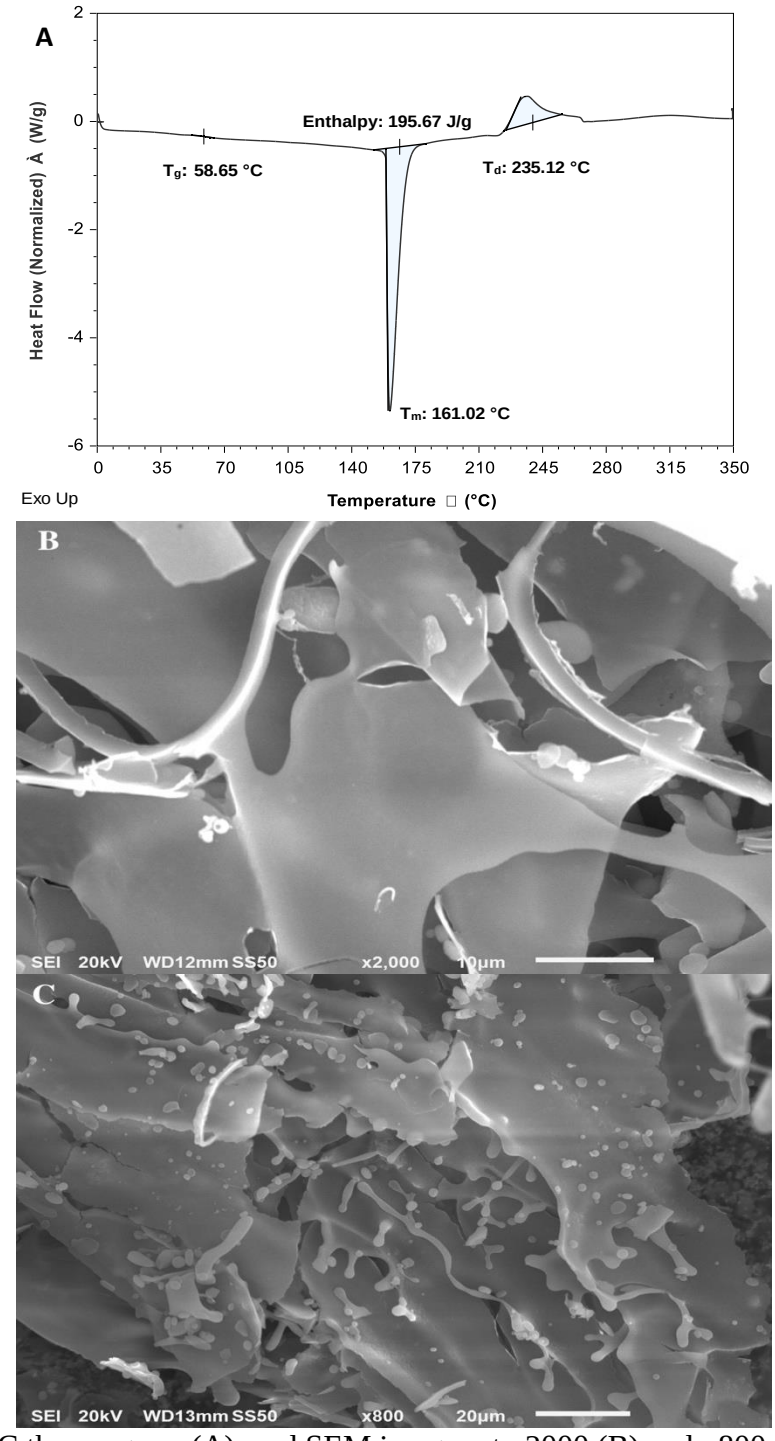

Figure 3: The DSC thermogram (A), and SEM images at x2000 (B) and x800 (C) magnifications of EPS-MS79

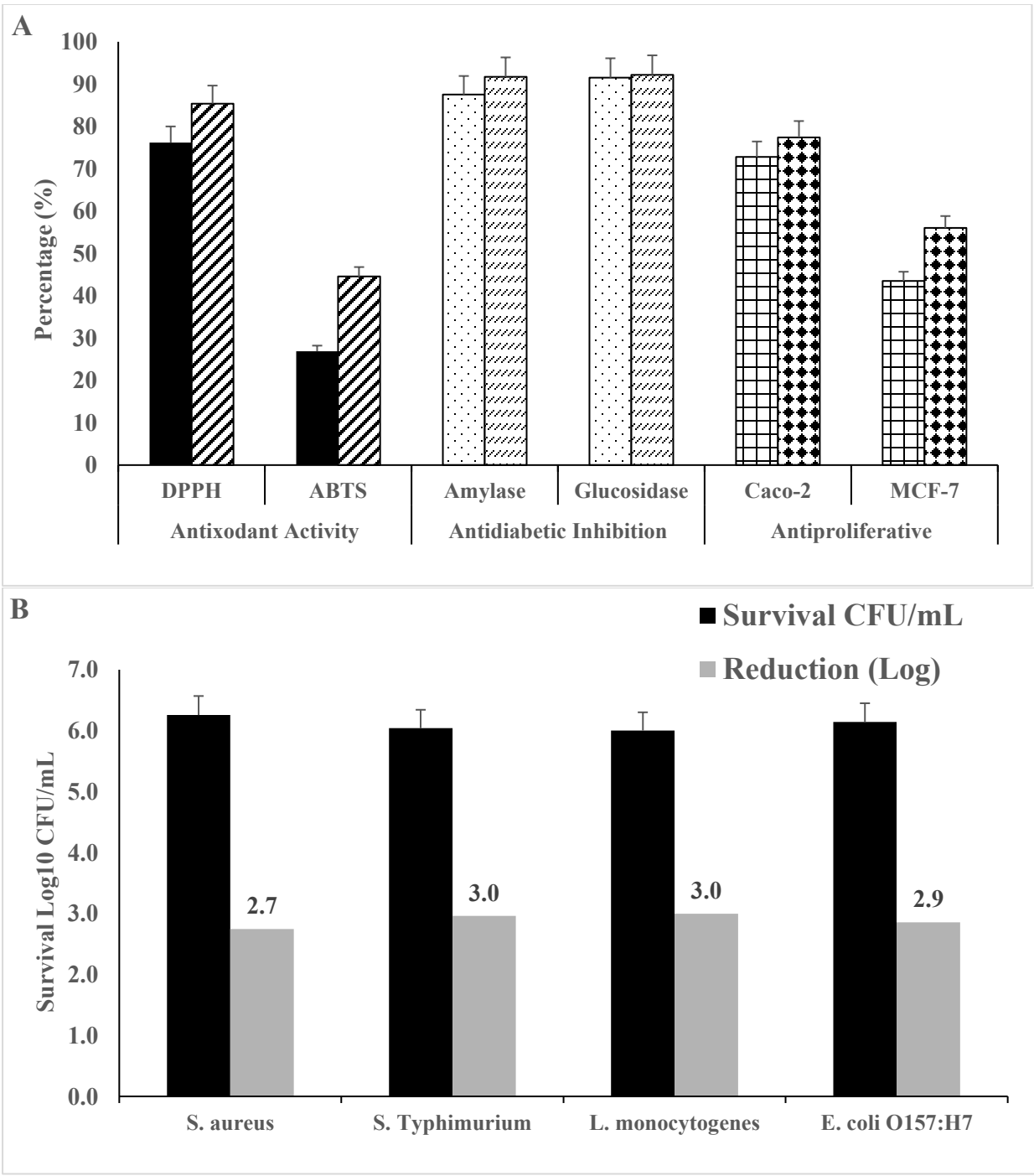

Figure 4: The bioactivities of EPS-MS79: (A) Antioxidant (5 mg ■ and 10 mg ▨), antidiabetic (100 µg ⬚ and 200 µg ▤) and antiproliferative activities (5 mg ▦ and 10 mg ▩). (B) Antibacterial activity

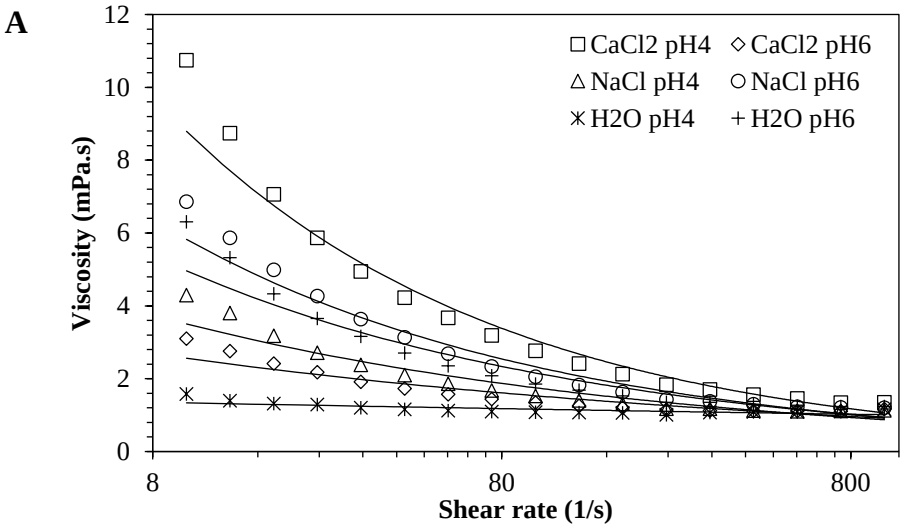

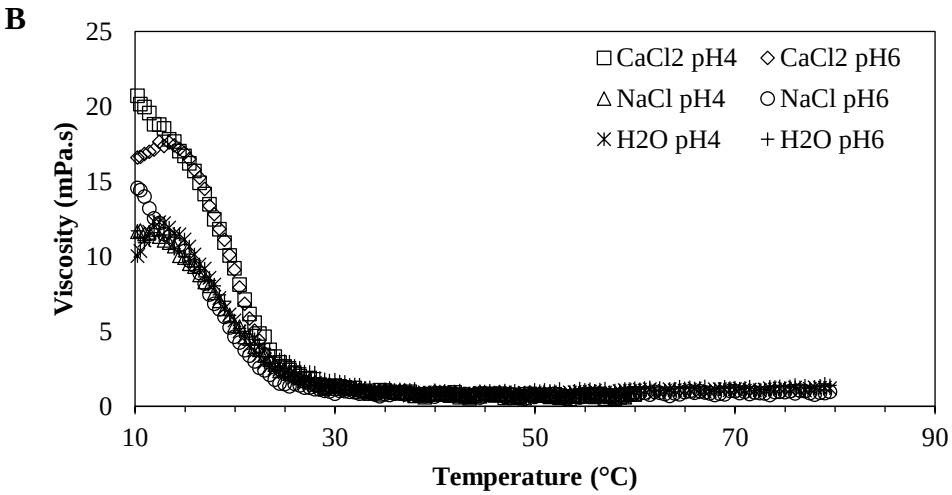

Figure 5: Apparent viscosity (A) and Temperature-dependent behavior (B) of EPS-MS79 solutions (5 mg) prepared with $CaCl_2$ pH 6.0 (◇), $CaCl_2$ pH 4.0 (□), NaCl pH 6.0 (○), NaCl pH 4.0 (△), H_2O pH 6.0 (+), or H_2O pH 4.0 (×).

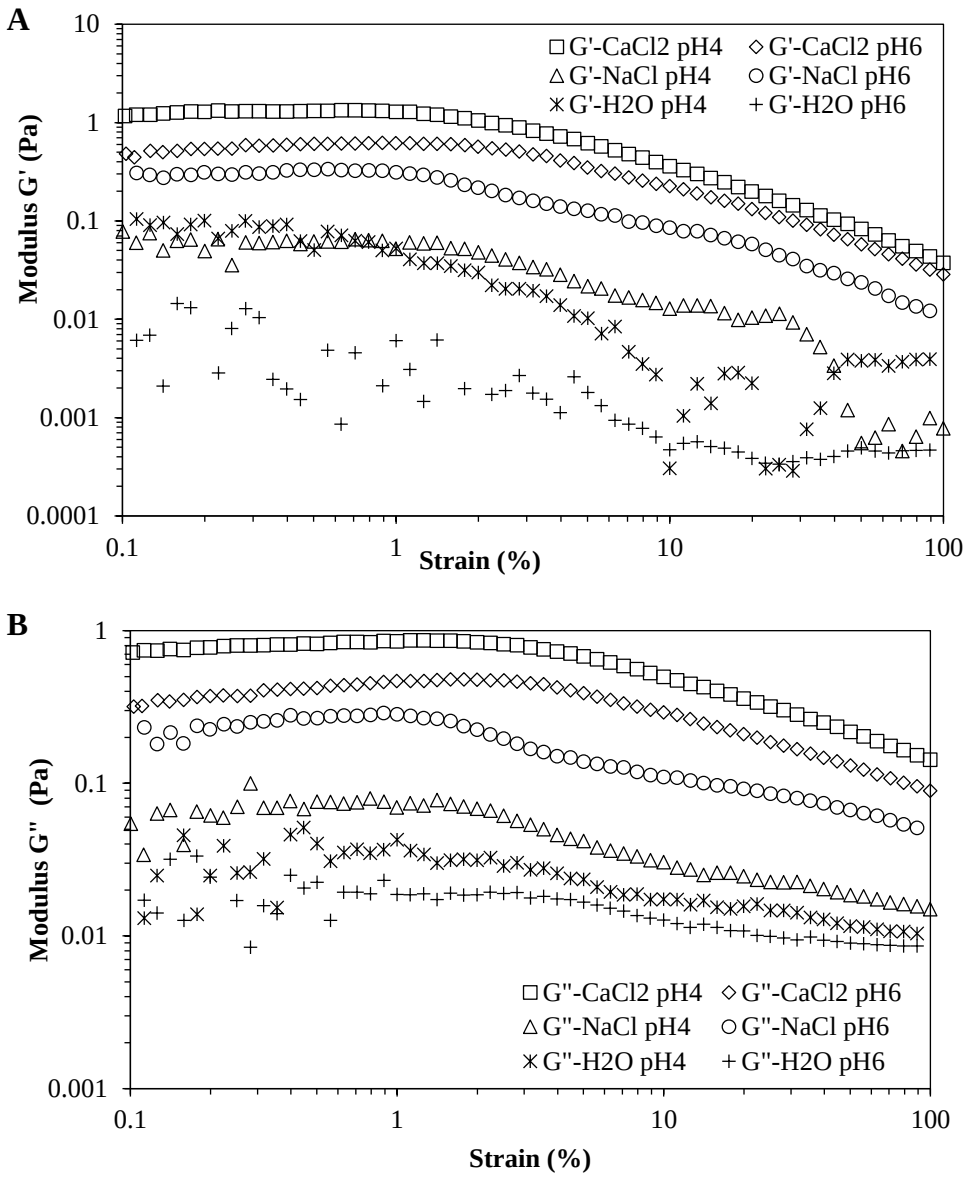

Figure 6: Storage G' (A) and loss G" (B) of EPS-MS79 solutions (5 mg) prepared with $CaCl_2$ pH 6.0 (◇), $CaCl_2$ pH 4.0 (□), NaCl pH 6.0 (○), NaCl pH 4.0 (△), H_2O pH 6.0 (+), or H_2O pH 4.0 (×).

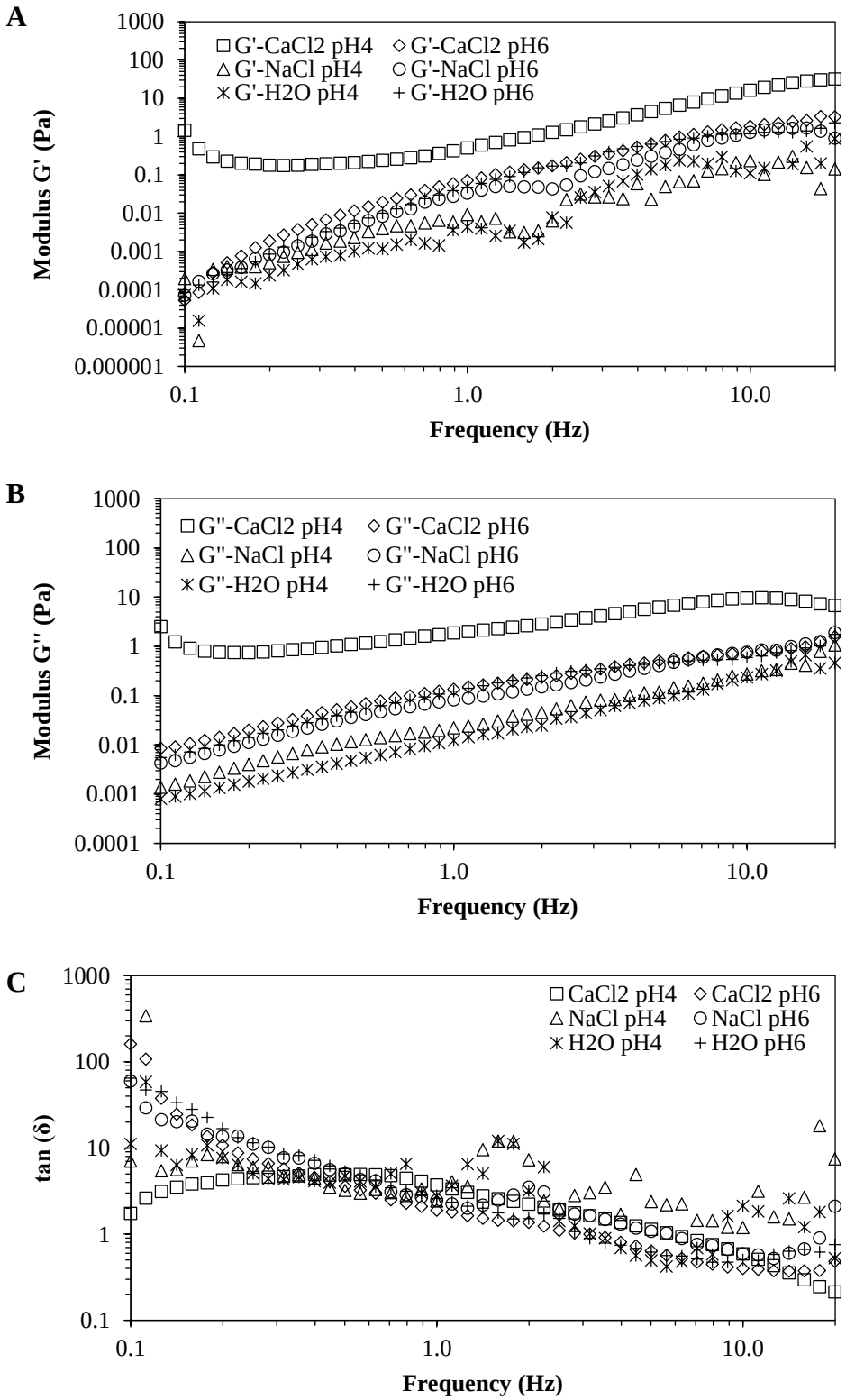

Figure 7: G' (A, elastic), G" (B, viscus), and tan delta (δ) of EPS-MS79 solutions (5 mg) prepared with $CaCl_2$ pH 6.0 (◇), $CaCl_2$ pH 4.0 (□), NaCl pH 6.0 (○), NaCl pH 4.0 (△), H_2O pH 6.0 (+), or H_2O pH 4.0 (×).

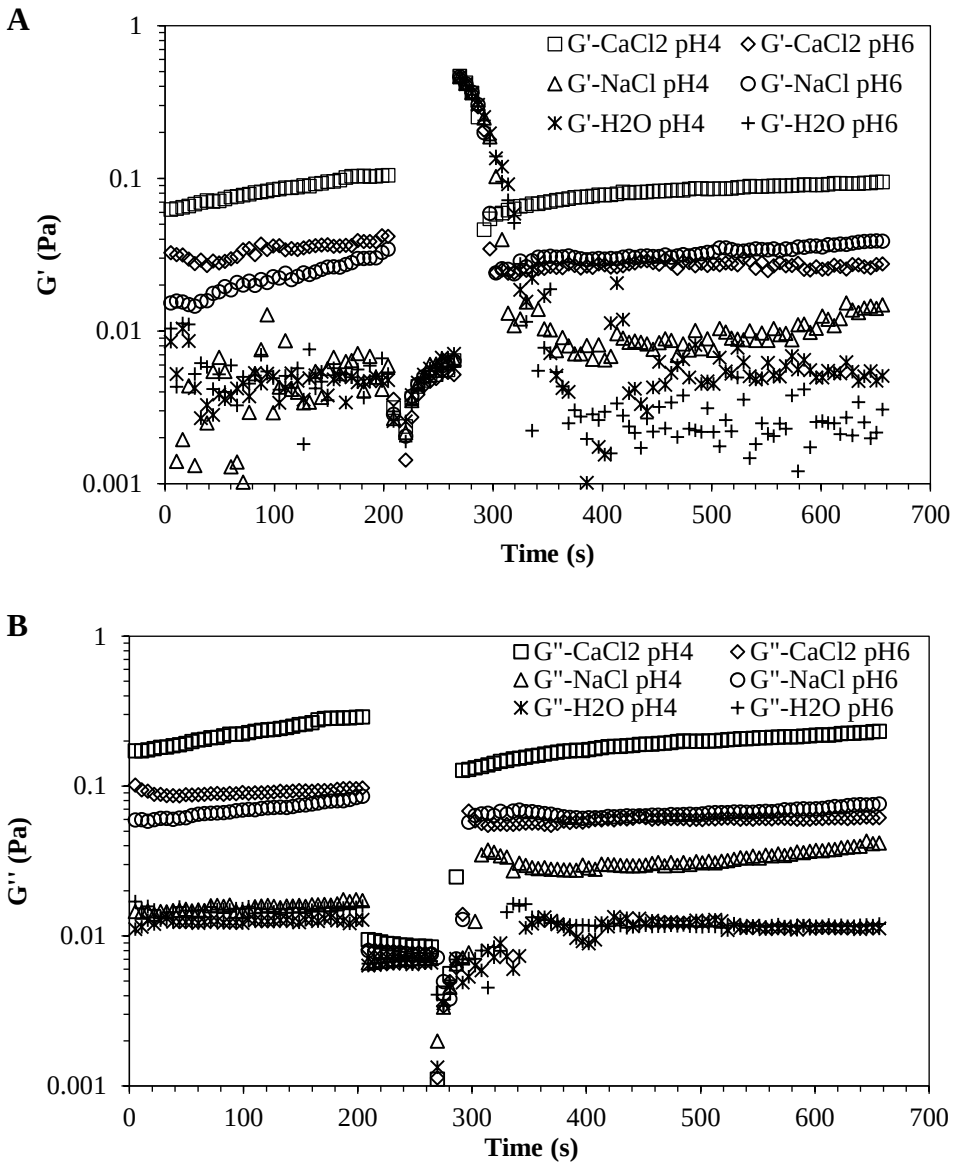

Figure 8: Thixotropic behavior of EPS-MS79 solutions (5 mg) prepared with $CaCl_2$ pH 6.0 (◇), $CaCl_2$ pH 4.0 (□), NaCl pH 6.0 (○), NaCl pH 4.0 (△), H_2O pH 6.0 (+), or H_2O pH 4.0 (×).